
Article:
Zhang, F, Wang, Y, Liu, Y et al. (6 more authors) (2019) Transcriptional Regulation of Voltage-Gated Sodium Channels Contributes to GM-CSF-Induced Pain. Journal of Neuroscience, 39 (26). pp. 5222-5233. ISSN 1529-2401

https://doi.org/10.1523/JNEUROSCI.2204-18.2019

Transcriptional regulation of voltage-gated sodium channels contributes to GM-CSF induced pain

Abbreviated title: the role of Nav1.7-1.9 channel in GM-CSF induced pain

Fan Zhang[1,2†], Yiying Wang[1†], Yu Liu[1,2], Hao Han[1], Dandan Zhang[2], Xizhenzi Fan[2], Xiaona Du[1], Nikita Gamper[1,3], Hailin Zhang[1*]

[1]Department of Pharmacology, Hebei Medical University; The Key Laboratory of Neural and Vascular Biology, Ministry of Education, China; The Key Laboratory of New Drug Pharmacology and Toxicology, Hebei Province; Shijiazhuang, China.

[2]Department of Biochemistry and Molecular Biology, Hebei Medical University, Hebei Province, Shijiazhuang, China.

[3]School of Biomedical Sciences, Faculty of Biological Sciences, University of Leeds, Leeds, UK

*Correspondence: Professor Hailin Zhang, Department of Pharmacology, Hebei Medical University, Shijiazhuang, China. 050017, E-mail: zhanghl@hebmu.edu.cn

[†]These authors contributed equally to this work

5 figures

1 table

Abstract: 185 words

Introduction: 671 words

Discussion: 924 words

Acknowledgments This work is supported by the National Natural Science Foundation of China (91732108 to HZ), (31872788 and 31401199 to FZ) and (31571088 to XD); Key Basic Research Project of Applied Basic Research Program of Hebei Province (16967712D to XD); Biotechnology and Biological Sciences Research Council (Grants BB/R003068/1 and BB/R02104X/1 to NG). We greatly appreciate the collection of human osteosarcoma and chondroma tissues from Prof. Yueping Liu (The Fourth Hospital of Hebei Medical University, China).

Conflict of interest There are no conflicts of interest.

Author Contributions YW, DZ, FX-Z, YL, HH and FZ performed the experiments and data analyses. HZ, FZ, XD and NG designed the experiments. HZ, FZ and NG wrote the paper. All authors have read, edited and approved the content of the manuscript.

Abstract

Granulocyte-macrophage colony stimulating factor (GM-CSF) induces production of granulocyte and macrophage populations from the hematopoietic progenitor cells; it is one of the most common growth factors in the blood. GM-CSF is also involved in bone cancer pain development by regulating tumor-nerve interactions, remodeling of peripheral nerves and sensitization of damage-sensing (nociceptive) nerves. However, the precise mechanism for GM-CSF-dependent pain is unclear. In this study, we found that GM-CSF is highly expressed in human malignant osteosarcoma. Female Sprague-Dawley rats implanted with bone cancer cells develop mechanical and thermal hyperalgesia but antagonizing GM-CSF in these animals significantly reduced such hypersensitivity. The voltage gated Na^+ channels Nav1.7, Nav1.8 and Nav1.9 were found to be selectively up-regulated in rat DRG neurons treated with GM-CSF, which resulted in enhanced excitability. GM-CSF activated the Jak2 and Stat3 signaling pathway which promoted the transcription of Nav1.7-1.9 in DRG neurons. Accordingly, targeted knocking down of either Nav1.7-1.9 or Jak2/Stat3 in DRG neurons in vivo alleviated the hyperalgesia in male Sprague-Dawley rats. Our findings describe a novel bone cancer pain mechanism and provide a new insight into the physiological and pathological functions of GM-CSF.

Significance Statement

It has been reported that GM-CSF plays a key role in bone cancer pain, yet the underlying mechanisms involved in GM-CSF-mediated signaling pathway in nociceptors is not fully understood. Here, we showed that GM-CSF promotes bone cancer-associated pain by enhancing excitability of DRG neurons via the Jak2-Stat3-mediated upregulation of expression of nociceptor-specific voltage-gated sodium channels. Our study provides a detailed understanding of the roles that sodium channels and Jak2/Stat3 pathway play in the GM-CSF-mediated bone cancer pain; our data also highlight the therapeutic potential of targeting GM-CSF.

Introduction

Granulocyte-macrophage colony stimulating factor (GM-CSF) was originally identified as a colony stimulating factor because of its ability to induce granulocyte and macrophage populations from precursor cells. GM-CSF is also abundantly secreted by some tumor cells and plays a key role in regulating tumor-nerve interactions, remodeling of peripheral nerves and sensitization of damage-sensing nerves (nociceptors) by acting at its receptors (Schweizerhof et al., 2009). Apart of the bone metastases pain, GM–CSF was also shown to be involved in inflammatory pain, arthritic and neuropathic pains (Cook et al., 2012; Cook et al., 2013; Nicol et al., 2018). A recent study show that GM-CSF signaling contributes to pain-associated behavior that is independent of a gliosis and/or astrocyte response, suggesting that GM-CSF may directly activate sensory neurons (Nicol et al., 2018). However, the precise mechanism for GM-CSF-dependent pain is unclear.

Dorsal root ganglion (DRG) neurons are the peripheral somatic and visceral sensory neurons; a subset of these neurons is responsible for nociceptive signal initiation and propagation. Receptors for GM-CSF (GM-CSFR) are found to be expressed in DRG and in peripheral nerves dispersed in the periosteum of mice (Schweizerhof et al., 2009). Signaling cascades and mechanisms of action of GM-CSFR in sensory neurons are largely unknown but in hematopoietic cells, activation of GM-CSFR is known to stimulate cell signaling pathways regulating gene expression, including the Jak-Stat pathway (Janus kinase, JAK; signal transducer and activator of transcription protein, Stat) (Stosser et al., 2011). Activation of Jak leads to dimerization and translocation of Stat family transcription factors to cell nucleus to regulate gene expression (Fortin et al., 2007). The main aim of the present study was to identify molecules involved in GM-CSF-mediated signaling pathway in nociceptors and test their relevance to GM-CSF-induced pain.

Ion channels are the basis of sensory neuronal excitability and were previously suggested as molecular targets of GM-CSF signaling pathway (Bali et al., 2013). Our preliminary screening (see Results and Figure 3-1) revealed that GM-CSF selectively increased expression in DRG neurons of three voltage-gated sodium channels, Nav1.7,

Nav1.8 and Nav1.9. Due to the primary role of these channels in the ability of DRG neurons to generate action potentials (APs), we hypothesized that GM-CSF might promote pain and hyperalgesia by acting on voltage-gated Na^+ channels in nociceptors.

At least five different voltage-gated sodium channels are reportedly expressed in DRG, including the TTX-sensitive Nav1.1, Nav1.6 and Nav1.7 and the TTX-resistant Nav1.8 and Nav1.9 (Cummins et al., 2000). Nav1.7, Nav1.8 and Nav1.9 channels are mainly distributed in small diameter DRG neurons, most of which are involved in nociception. Nav1.7 produces a rapidly-activating and inactivating but slowly repriming current. It produces a robust ramp current in response to depolarizations, contributing to the generation and propagation of action potentials and acting as a threshold channel regulating excitability (Francois-Moutal et al., 2018; Li et al., 2018). Gain-of-function mutations within the Nav1.7 gene SCN9A lead to inherited pain disorders, such as erythromelalgia (IEM) and paroxysmal extreme pain disorder (PEPD) (Dib-Hajj et al., 2008; Jarecki et al., 2010; Cheng et al., 2011). Nav1.8 mediates a slowly-inactivating sodium currents acting as a key component of the upstroke of the action potential and thus influences neuronal excitability and nociceptive transmission. Mutations of Nav1.8 gene, SCN10A, is found in patients with peripheral neuropathy (Lai et al., 2002; Choi et al., 2007; Blanchard et al., 2012). The Nav1.9 channel has a slow kinetics and is responsible for persistent Na^+ currents in nociceptors; together with the Nav1.7 it acts as a threshold channel for AP firing; it amplifies sub-threshold stimuli leading to AP bursts (Huang et al., 2014). Gain-of-function mutations of Nav1.9 channel gene, SCN11A cause familial episodic pain syndrome (Huang et al., 2014; Huang et al., 2017).

In this study, we found that GM-CSF significantly increased the excitability of DRG neurons in parallel with the increase the current density, mRNA and protein expression of Nav1.7, Nav1.8 and Nav1.9 channels. We further show Jak2-Stat3-mediated up-regulation of Nav1.7, Nav1.8 and Nav1.9 channel expression in nociceptors is a major factor in the GM-CSF-related component of bone cancer pain.

Materials and methods

Human subjects. The study was carried out in accordance with the ethical principles for medical research involving human subjects set out in the Helsinki Declaration, and was approved by the ethical committee at Hebei Medical University (Shijiazhuang, China). Osteosarcoma or chondroma tissues were obtained from 8 patients from the Fourth Hospital of Hebei Medical University. Each specimen was fixed with 4% paraformaldehyde for immunohistochemistry study. All patients or their relatives gave informed consent prior to their participation in the study.

Animals. The animal protocols used in this study were approved by the Animal Care and Ethical Committee of Hebei Medical University under the International Association for the Study of Pain (IASP) guidelines for animal use. All surgeries were performed under sodium pentobarbital (Sigma) anesthesia, and all efforts were made to minimize animal suffering.

Rat DRG neuron culture. Dorsal root ganglion (DRG) neurons were obtained from adult Sprague-Dawley rats (provided by Experimental Animal Center of Hebei Province) based on the protocol described previously (Du X et al., 2014). Briefly, the ganglia were digested at 37°C with collagenase (2 mg/ml) with dispase (7.5 mg/ml) for 30 min. Ganglia were then mechanically triturated and washed twice with DMEM supplemented with 10% fetal calf serum. Thereafter, the DRG neurons were plated on poly-D-lysine-coated glass cover slips.

Quantitative PCR. Total RNA was extracted using a commercial RNA isolation kit (RNAiso, Takara). Isolated RNA was dissolved in 20 μl DEPC-treated water and reverse-transcribed using an RT reagent kit (PrimeScript with gDNA Eraser, Takara) and a thermal cycler (Mastercycler, Eppendorf). Quantitative PCR reaction was

performed using a kit (SYBR Premix Ex TaqII [Tli RNase H Plus], Takara), and the fluorescent DNA was detected and quantified with an FQD-48A(A4) system (BIOER). The PCR products were also run on a 2% agarose gel and were visualized using a gel imager (TFP-M/WL, Vilber Lourmat). For qPCR analysis, the following specific primers were used:

Nav1.7-Forward: GCTCCAAGGACACAAAACGAAC,

Nav1.7-Reverse: ATCAGACTCCCCAGGTGCAAT;

Nav1.8-Forward: GACCCTTTCTACAGCACACACC,

Nav1.8-Reverse: AAGTCCAGCCAGTTCCACG;

Nav1.9-Forward: GCCCCTTCACTTCCGACT,

Nav1.9-Reverse: GTCTTCCAGAGGCTTCGCTAC;

GAPDH-Forward: CCAGCCTCGTCTCATAGACA,

GAPDH-Reverse: CGCTCCTGGAAGATGGTGAT

Luciferase reporter assay. The Stat3 luciferase reporter vector was designed to measure the binding of transcription factors to the enhancer, and was transfected into HEK293 cells with Lipofectamine2000 reagent (Invitrogen).

Fragments of rat Scn9a, Scn10a and Scn11a gene were amplified by PCR with following primers:

Forward-GGCTCGAGAGCTTAAGGAAAGGAGGGTA,

Reverse-GTAAGCTTTTTCCCCTTTGACTCCTTAC; corresponding to the promotor region of Scn9a (-286/+306).

Forward-GGCTCGAGCCGTAGTAAGACCCTGCCTTG,

Reverse-GTAAGCTTGAGACCCCAGCTCTGCAAAAC; corresponding to the promotor region of Scn10a (749/+124) .

Forward-GGCTCGAGCTTCACATGGTTGATCCATC

Reverse-GTAAGCTTATTCTCGCTCTTGGCAGTA; corresponding to the promotor region of Scn11a (-51/+556 regions).

Amplified fragments were digested with appropriate restriction enzymes and cloned into pGL3 Basic (Promega). Luciferase activity was measured using a Dual Luciferase Assay Kit (Promega). Specific promoter activity was expressed as the relative activity ratio of firefly luciferase to Renilla luciferase.

Western Blot. The DRG neuron lysates were prepared with RIPA lysis buffer. Equal amounts of protein were separated by sodium dodecyl sulfate polyacrylamide gel electrophoresis (SDS-PAGE) and electrotransferred to a polyvinylidene fluoride membrane. Membranes were blocked with 5% non-fat dairy milk and incubated with primary antibodies against Nav1.7 (1:500, Alomone), Nav1.8 (1:500, Abcam), Nav1.9 (1:200, Abcam), p-Jak1 (1:1000, Affinity), p-Jak2 (1:1000, Affinity), p-Jak3 (1:1000, Affinity), p-stat3 (1:1000, Epitomics), p-Stat5a (1:1000, Affinity) at 4°C overnight. This was followed by incubation with IRDye800-conjugated secondary antibody (1:20,000, Rockland) for 1 h at room temperature and subsequent scanning with the Odyssey Infrared Imaging System (LI-COR Biosciences). The integrated intensity for each detected band was determined using Odyssey Imager software (v3.0).

Immunohistochemistry. Sections from human osteosarcoma or chondroma tissues were blocked with 0.3% hydrogen peroxide, followed by preincubation with 5% normal goat serum and then incubation with primary antibodies against GM-CSF (1:200, Pepro Tech) at 4 °C overnight. Next, the sections were incubated with the biotinylated secondary antibody, followed by streptavidin-horseradish peroxidase and diaminobenzidine, and then counterstained with hematoxylin. Staining intensities were determined by measurement of the integrated optical density (IOD) by light microscopy using a computer-based Image-Pro Morphometric System.

Electrophysiology. Action potentials were recorded from dissociated rat small diameter DRG neurons (<25 μm) under current clamp using an Axopatch 200B amplifier and a Digidata 1322A converter (Axon Instruments). Pipettes (3–4 MΩ) were filled with solution containing (in mM): KCl 150, $MgCl_2$ 5, HEPES 10, pH 7.4 adjusted with KOH. The bath solution contained (in mM): NaCl 160, KCl 2.5, $MgCl_2$ 1, $CaCl_2$ 2, glucose 10, HEPES 20 and pH 7.4 adjusted with NaOH. Small DRG neurons were examined for evoked activity with a series of 1-s current injections from 0 pA to 500 pA in 50 pA increments. The rheobase currents were determined by the first action potential elicited by a series of depolarizing current injections that increased in 5 pA increments. The following values were measured in this study: resting membrane potential (RMP), threshold potential (TP), AP amplitude, depolarization rate (V/s).

Sodium currents were recorded from these small diameter DRG neurons under the voltage clamp mode in a whole-cell configuration. Pipettes (3–4 MΩ) were filled with solution containing (in mM): 70 CsCl, 30 NaCl, 30 TEA-Cl, 10 EGTA, 1 $CaCl_2$, 2 $MgCl_2$, 2 Na_2ATP, 0.05 GTP, 10 HEPES, and 5 glucose, pH 7.3 with CsOH. The bath solution for DRG neurons was (in mM): 80 NaCl, 50 choline-Cl, 30 TEA-Cl, 2 $CaCl_2$, 0.2 $CdCl_2$, 10 HEPES, and 5 glucose, pH 7.3 with NaOH. The acquisition rate was 20 kHz and signals were filtered at 5 kHz. Series resistances were compensated by 80%. Currents were elicited by a 40 ms pulses from a holding potential of -120 mV to test potentials between -80 mV and +40 mV in 5 mV increments. The TTX-resistant (TTX-R) sodium currents (including both Nav1.9 and Nav1.8 currents) were recorded in the presence of 300 nm TTX in the external solution. The TTX-sensitive (TTX-S) sodium currents were obtained by digital subtraction of the TTX-R sodium currents from the total currents. Nav1.8 currents were then elicited by a prepulse of -70 mV for 500 ms before the test potentials from -80 mV to +40 mV in 5 mV increments in the same neuron. The Nav1.9 currents were obtained by digital subtraction of the Nav1.8 currents from the TTX-R sodium currents (based on protocols from（Qiu et al., 2016).

Rat model of tumor-evoked pain. The Walker 256 carcinosarcoma breast cancer cells were provided by Shanghai Cell Bank of the Chinese Academy of Sciences. Wistar rats were injected intra-peritoneally with the Walker 256 cancer cells 0.5 ml (2×10^7 cells/ml and 6–7 days later ascitic fluid was extracted. Sprague Dawley rats (180-200 g) were anesthetized by intraperitoneal injection of sodium pentobarbital (60-80 mg/kg). The right leg was shaved and the skin was disinfected with 70% (v/v) ethanol. A 1-cm-long rostro-caudal incision was made in the skin over the lower one-third of the tibia for exposure with minimal damage to muscles and nerves. The medullary canal was approached by inserting a 23-gauge needle proximally through a hole drilled in the tibia. The needle was then replaced with a 10-μl microinjection syringe containing the cells to be injected. A 5-μl volume of Walker 256 cells (4×10^6/ml) or boiled cells (sham group) were injected into the bone cavity. After a 2-min delay to allow cells to fill the bone cavity, the syringe was removed and the hole was sealed using bone wax. In some experiments, antibody against GM-CSF (10 μg, SCBT), antibody GM-CSFR (10 μg, SCBT), GM-CSF antagonist, E21R (25 μg/μl, 3 μl, Life Tein LLC) or vehicle was injected in the vicinity of the tibia bone. The wound was closed using 1-0 silk threads and dusted with penicillin powder. The rats were allowed unrestricted movement in their cages after recovery and their general condition was monitored during the experiment.

Focal application of drugs to DRG in vivo. All surgical procedures were performed under deep anesthesia with an i.p. injection of pentobarbital sodium (60-80 mg/kg). A DRG cannula for focal application of substances to DRG was implanted as previously described (Du X et al., 2017). Briefly, a midline incision was made at the L4-L6 spinal level of adult male rats (Sprague Dawley; 180-200 g), and the L5 was identified at the midpoint of a link between both sides of the iliac crest. A 0.8-mm hole (~1 mm off the inferior edge of the transverse process) was drilled through the transverse process over the L5 DRG. Approaching of a ganglion was verified by the twitch of the paw. A hooked stainless steel blunt-tip cannula (inner diameter 0.64 mm, length 4 mm) was forced into the hole and connected to a polypropylene tube (inner

diameter 0.41 mm, length 4.5 mm). The incision was closed with sutures, and the cannula was firmly fixed in place with dental cement. Intramuscular injection of benzylpenicillin (19 mg/0.1 ml) was given immediately after surgery. Postoperatively, rats were housed individually in plastic cages with sawdust flooring and supplied with water and food ad libitum. Animals were left to recover for at least 24 hours before the experiments were carried out. Animals developing signs of distress were humanely sacrificed.

Antisense oligonucleotide knockdown. On the second day after DRG cannula implantation, rats were given through the cannula the antisense oligodeoxynucleotides (AS ODNs) against Scn9a, Scn10a, Scn11a, Jak2, Stat3 or Stat5 (each at 12.5 μg in 5 μl). The AS ODNs were given consecutively twice a day for 4 days. Mismatched ODNs were also given at matched time points. On the fifth day, mechanical and thermal sensitivities were assessed at 1 h, 2 h, 5 h, 12 h, and 24 h after the focal DRG application of GM-CSF (5 μl) or saline (5 μl) , respectively. Seven groups of animals were tested, injected as follows:

Group	type of ODN pre-treatment	treatment type
1	mismatched ODN	GM-CSF or saline
2	AS ODN Scn9a	GM-CSF or saline
3	AS ODN Scn10a	GM-CSF or saline
4	AS ODN Scn11a	GM-CSF or saline
5	AS ODN Jak2	GM-CSF or saline
6	AS ODN Stat3	GM-CSF or saline
7	AS ODN Stat5a	GM-CSF or saline

The following specific ASO were used:

Mismatched ODN: TCACCCAGCACCCCCAACACATAGTT

ASO- Scn9a: CTGGATCAACATGGTCTTCA

ASO- Scn10a: CCAGAACCAAGCACAGAGGA

ASO- Scn11a: CACCATCTGCATCATCATCA

ASO-Jak2: AAGGTACAGATTCCGCAGGT

ASO-Stat3:ACATGGAGGAGTCCAACAAC

ASO-Stat5a:TCTCAGTTCAGCGTTGGCAG

Mechanical hyperalgesia. Threshold sensitivity to mechanical stimuli was assessed using the von Frey method as described previously (Chaplan et al., 1994). Briefly, calibrated nylon filaments (Von Frey hair, Stoelting Co,) with different bending forces were applied to the midplantar surface of the right hind paw of the rats. The filaments were applied starting with the softest and continuing in ascending order of stiffness. A brisk withdrawal of the right hind limb was considered a positive response.

Thermal hyperalgesia. The paw withdrawal latency in response to heat was tested using the Hargreaves method on the right hind paw of the rats using a radiant heat lamp source (Mengtai Technology Co., Ltd.). The intensity of the radiant heat stimulus was maintained at 20%. The time to withdrawal of the right hind paw (elapse time) was recorded.

Blinding and randomization. In all in vivo experiments when animal behavior test and drug administration were involved, experiments were conducted on the basis of a blind and randomized design. To achieve this, two experimenters performed every tests: one experimenter was in charge of drug injections and group randomization; second experimenter, blinded to the drug administration and grouping

schedules, conducted the mechanical and thermal sensitivity measurements.

Statistics and analysis. All data are given as mean ± SEM. Differences between groups were assessed by paired or unpaired t test. Comparisons of the behavioral data between groups at each individual time point were conducted using a two-way ANOVA followed by Bonferroni post hoc tests. Comparisons of the number of action potential between groups at each injected currents were conducted using a two-way ANOVA followed by Bonferroni post hoc tests. Differences were considered significant at $P \leq 0.05$. Statistical analyses were performed using OriginPro 9.1 (Originlab Corp.).

Results

GM-CSF plays a crucial role in bone metastases cancer pain. Osteosarcoma is the most common form of primary bone cancer, in which pain is the most common symptom and is seen in 85% of patients (Yoneda et al., 2015). Osteochondroma is the most common benign bone tumor and the majority of osteochondromas form an asymptomatic hard immobile painless palpable mass (de Mooij et al., 2012). We first collected tumor tissue from osteosarcama and osteochondroma patients after surgery, and compared the expression levels of GM-CSF in these two tumor tissue types. The H&E staining shows typical characteristics of a cancerous (Fig. 1A, low left) and a benign (Fig. 1A upper left) bone tissue. Interestingly, osteosarcoma biopsy samples demonstrated a dramatically increased levels of GM-CSF, as compared to these seen in osteochondroma samples, as revealed with immunohistochemistry (Fig. 1A right panels; summarized in Fig. 1B, $n = 8$, $^*P < 0.05$).

To explore the role of GM-CSF in bone cancer pain, we first established the bone metastases cancer pain model induced by the implanted Walker 256 carcinoma cells. Consistent with previous reports (Wang et al., 2011), mice with tumors in the tibia bone displayed a significantly lower withdrawal thresholds for mechanical stimuli and a shortened withdrawal latencies for thermal stimuli at 3-21 days after tumor cell

injection (Fig. 1C, 1D). To assess the role of GM-CSF in these behavioral manifestations of pain hypersensitivity, we injected a mutant GM-CSF peptide with the glutamate-to-arginine substitution at the position 21 of a rat GM-CSF peptide sequence (E21R). E21R acts as a competitive antagonist of GM-CSF and can neutralize some of its biologic actions (Iversen et al., 1996), however its effect on GM-CSF-mediated pain has not been tested before. E21R was injected in the vicinity of the tibia bone where the cancer cells had been implanted (see Methods). Treatment of the bone cancer rats with E21R significantly alleviated both mechanical and thermal hyperalgesia, respectively (Fig. 1C). The reduction of hyperalgesia was registered starting from day 7 after the establishment of the bone cancer model and lasted for the duration of observation (21 days). To further validate the role of GM-CSF in the bone cancer pain, we also used antibodies against GM-CSF and GM-CSF receptor (GM-CSFR). Injection of anti-GM-CSF and anti-GM-CSFR antibodies also produced strong anti-hyperalgesic effect, the anti-GM-CSFR antibody was particularly efficacious, resulting in significantly stronger anti-hyperalgesia, as compared to E21R (Fig. 1C). These results indicate that GM-CSF is indeed involved in the bone cancer pain development, which is in agreement with a previous report that the bone cancer pain was attenuated following a specific knockdown of GM-CSF receptors in L4-L5 DRG of mice (Schweizerhof et al., 2009).

To further attest that GM-CSF is pro-algesic and the primary afferent sensory nerve are the targeted sites of GM-CSF action, we evaluated the effect of direct focal GM-CSF infusion into the L5 DRG on pain-related behavior in naïve rats (Fig. 1D). Compared with the vehicle-treated rats, GM-CSF induced significant dose-dependent thermal and mechanical hyperalgesia which persisted for at least 24 hrs after injection. Indeed, focal injection of GM-CSF (20 - 200 ng) via the DRG cannula significantly increased sensitivity of rats to thermal and mechanical stimuli as measured with the Hargreaves and Von Frey tests, respectively ($P < 0.05$). The nociceptive responses in rats received 2 ng of GM-CSF also showed a tendency towards sensitization but these effects did not reach statistical significance.

GM-CSF increase the excitability of small-sized DRG neuron. The fact that GM-CSF enhanced pain sensitivity when injected into DRG suggests that GM-CSF might directly sensitize nociceptors by increasing their excitability. To test this hypothesis, we performed current clamp recordings from the cultured DRG neurons in control conditions and after 24 hrs treatment with GM-CSF (200 ng/ml). For this study, small diameter (< 25 μM) DRG neurons were selected as these are predominantly nociceptors (Zheng et al., 2013). AP firing was induced by trains of depolarizing current step from +50 to +500 pA, injected with a 50 pA increment. GM-CSF significantly increased the number of APs induced by the depolarizing current pulses from 100 to 500 pA (Fig. 2A, B). GM-CSF also significantly lowered the rheobase currents (depolarization current threshold (CT) for eliciting the 1st action potential) from 198.6 ± 9.8 pA (n = 63) to 83.1 ± 2.5 pA (n = 39, $P < 0.05$); the action potential threshold voltage (TP) was also significantly decreased from -18.7 ± 0.5 mV (n = 23) to -20.4 ± 0.6 mV (n = 22, $P < 0.05$). However, the resting membrane potential was not significantly changed (Fig. 2C, 1D). We also measured the effect of GM-CSF treatment on other properties of evoked APs such as AP amplitude (mV) and rate of depolarization (V/s), which are summarized in Table 1. Together, the above data indicate that GM-CSF increases intrinsic neuronal excitability of primary sensor neurons associated with pain.

GM-CSF increases activity and expression level of Nav1.7 Nav1.8 and Nav1.9 sodium channels. The sensitizing effect of a single focal in vivo injection of GM-CSF was long-lasting (Fig. 1E), in addition, intracellular action of GM-CSFRs has long been linked to transcriptional effects via the activation of Jak-Stat pathway. Thus, we hypothesized that the sensitizing effect of this growth factor might be mediated by changes in the expression of some intrinsic regulator(s) of excitability. Thus, to further explore the mechanisms for GM-CSF-induced hyperactivity of DRG nociceptors, we screened the effect of GM-CSF on ion channels which have been implicated in modulation of resting excitability of DRG neurons (Liu et al., 2010; Zheng et al., 2013; Qiu et al., 2016; Isensee et al., 2017; Du et al., 2018). We tested

the effect of treatment of cultured DRG neurons with 200 ng/μl GM-CSF (24 hrs) on the mRNA abundance of the following ion channel genes: Scn9a (Nav1.7), Scn10a (Nav1.8), Scn9a (Nav1.9), Kcnd2 (Kv4.2), Ano1 (TMEM16A), P2rx3 (P2X3), Kcng2 (Kv7.2), Kcnq3 (Kv7.3). Among the transcripts tested, only the mRNAs of voltage-gated sodium channels Nav1.7, Nav1.8 and Nav1.9 were elevated (Figure 3A). Additionally, the mRNAs of Nav1.7-1.9 expression were elevated by day 7 in DRGs from bone cancer rats relative to those from sham controls (Figure 3B).

Next, we examined the effects of GM-CSF treatment on the current density of voltage-gated sodium currents in DRG neurons. Total, TTX- sensitive (TTX-S) and TTX-resistant Na^+ currents were recorded (see Method) using whole-cell patch clamp. After pretreatment of DRG neurons with GM-CSF (200 ng/ml; 24hrs), the peak current density of total Na^+ currents was increased from -101.0 ± 8.8 (pA/pF) (n = 44) to -155.8 ± 9.9 (pA/pF) (n = 32) at -10 mV; the peak current density of TTX-S currents (mainly Nav1.7 currents) was increased from -58.0 ± 6.5 (pA/pF) (n = 66) to -100.6 ± 4.7 (pA/pF) (n = 43) at -20 mV; the peak current density of TTX-R currents was increased from -56.5 ± 4.9 (pA/pF) (n = 66) to -75.5 ± 5.7 (pA/pF) (n = 43) at -10 mV (Fig 3C).

The TTX-R Na^+ currents were further separated into Nav1.8-rich currents and Nav1.9-rich current fractions (see Method). After pretreatment of DRG neurons with GM-CSF, the peak current density of Nav1.8-rich current fraction was increased from -44.5 ± 4.5 (pA/pF) (n = 55) to -60.1 ± 4.4 (pA/pF) (n = 36) at 0 mV; the Nav1.9-rich current fraction was increased from -20.2 ± 1.4 (pA/pF) (n = 53) to -29.4 ± 0.9 (pA/pF) (n = 36) at -20 mV (Fig. 3C). In sum, GM-CSF significantly increased the current amplitudes of nociceptor-specific Nav1.7 Nav1.8 and Nav1.9 currents. Furthermore, the protein expression levels of Nav1.7, Nav1.8 and Nav1.9 channel in DRG neurons were also significantly increased after incubation with GM-CSF (200 ng/ml; 18 h; Fig. 3D).

Down-regulation of Nav1.7-Nav1.9 channels alleviates GM-CSF induced pain. To investigate whether the up-regulation of Nav1.7, Nav1.8 and Nav1.9 channels

contributes to the GM-CSF-mediated pain, we performed unilateral in vivo knockdown of individual sodium channel subunit in rats using the anti-sense oligodeoxynucleotides (AS ODNs). AS ODNs against Scn9a, Scn10a and Scn11a (or a control mismatched ODN) were injected into the L5 DRG via the DRG cannula to offset the up-regulation of these sodium channels, and then the effect of GM-CSF on pain behavior was examined. The knockdown efficiency was measured first; for this, the L5 DRGs were extracted following focal injection of saline, GM-CSF, AS ODN + Saline, AS ODN + GM-CSF, and then the mRNA expression levels of Scn9a, Scn10a and Scn11a were analyzed by quantitative PCR. In agreement with previous data, the mRNA expression levels of Scn9a, Scn10a and Scn11a in DRG neurons were significantly increased after GM-CSF injection, and importantly, these increase were totally reversed by respective AS ODNs (Fig. 4A). Consistent with our earlier conclusion that up-regulation of Na1.7-Nav1.9 channels is a crucial factor in GM-CSF-induced hypersensitivity, AS ODNs against Scn9a, Scn10a and Scn11a significantly alleviated both mechanical and thermal hypersensitivity developed after the focal DRG application of GM-CSF (Fig. 4 B-C).

GM-CSF up-regulates Nav1.7-Nav1.9 channel expression via the Jak2-Stat3 signaling pathway. GM-CSF receptor is abundantly expressed in DRG (Schweizerhof et al., 2009). Thus we hypothesized that the GM-CSF induced up-regulation of Nav1.7-Nav1.9 in DRG neurons could be mediated by the GM-CSF receptor and the related cellular signaling pathway. To test this, we focused on the Jak-Stat3/5 pathway since this is the key pathway for GM-CSF action in hematopoietic cells (Lilly et al., 2001). Activated and phosphorylated states of Jak1, Jak2, Jak3, Stat3 and Stat5 were first measured in DRG neurons. As shown in Fig. 5A, after incubation of DRG cultures with GM-CSF for 25 min, phosphorylated Jak2 and Stat3 were significantly increased, but the level of phosphorylated Jak1 was not changed; phosphorylated Jak3 and Stat5 were not detected. These results indicate that GM-CSF is able to activate Jak2-Stat3 signaling pathway in DRG neurons. Is this activated Jak2-Stat3 signaling pathway responsible for GM-CSF–induced up-regulation of Nav1.7-Nav1.9 in DRG

neurons? To test this, the acutely disassociated DRG neurons were incubated with GM-CSF with and without blockers of Jak2-Stat3 signaling pathway, AG490 (10 μM) and stattic (20 μM). Both compounds prevented up-regulation Nav1.7-Nav1.9 mRNA by GM-CSF (Fig 5B).

As Stat3 was previously demonstrated to function as a transcriptional activator (Sharma et al., 2018), thus, we designed a luciferase reporter assay to determine if Stat3 acts to regulate Nav1.7-Nav1.9 transcription. Scn9a-Scn11a promoter regions (relative to the transcription start site) were cloned into a luciferase reporter vector (pGL3 Basic plasmid), such that luciferase expression is driven by either of the Scn9a-Scn11a promoter sequences. We transfected these DNA constructs and either a control pcDNA3.1 plasmid or a pcDNA3.1-stat3 plasmid into HEK293 cells and measured the resulting luciferase activity. Luciferase activity in cells co-expressed with Scn9a, Scn9a or Scn11a promoter fragments and Stat3 was 1.57 ± 0.14 ($n = 4$, $P < 0.05$), 1.5 ± 0.05 ($n = 4$, $P < 0.05$), 1.5 ± 0.15 ($n = 4$, $P < 0.05$) folds higher than that in cells co-expressed with Scn9a, Scn9a or Scn11a promoter fragments and the control pcDNA3.1 plasmid (Fig. 5C). These results implicate an important role for Stat3 in promoting Nav1.7, Nav1.8, and Nav1.9 gene expression.

Finally we assessed whether down regulation of Jak2-Stat3 signaling pathway would inhibit GM-CSF-induced up-regulation of Nav1.7-Nav1.9 and subsequently the pain behaviors. To this end, AS ODNs against Jak2 and Stat3 were injected in DRG (L5) via DRG cannula as described above. AS ODNs against Jak 2 (Fig. 5D) and Stat3 (Fig. 5E) but not against Stat5 (Fig. 5F) reduced basal mRNA levels of Scn9a-Scn11a and reversed the GM-CSF-induced up-regulation of Scn9a-Scn11a mRNA levels. Consistent with these results, AS ODNs against Jak2 (Fig. 5G) and Stat3 (Fig. 5H) but not AS ODNs against Stat5 (Fig. 5I) prevented the development of the mechanical and thermal hyperalgesia produced by focal in vivo application of GM-CSF via the DRG cannula (Fig. 5G, H, I). AS ODNs against Jak2, Stat3 and Stat5 did not significantly affect the mechanical and thermal sensitivity in rats without GM-CSF treatment (in accord with previous findings suggesting that Nav1.7, Nav1.8 or Nav1.9 knockout or knockdown does not significantly affect threshold

sensitivity in mice (Minett et al., 2013; Miao et al., 2010; Lolignier et al., 2011). Taken together, these results identified Jak2-Stat3-mediated up-regulation of Nav1.7-Nav1.9 channels as a key signaling pathway involved in the development of GM-CSF induced pain.

Discussion

In this study we demonstrate that GM-CSF promotes bone cancer-associated pain by enhancing excitability of DRG neurons via the Jak2-Stat3-mediated upregulation of expression of nociceptor-specific voltage-gated sodium channels. First, we show that GM-CSF is highly expressed in osteosarcoma biopsy samples from human patients. Second, we demonstrate that the competitive antagonist of GM-CSF, GM-CSF (E21R) as well as the antibodies against GM-CSF or GM-CSFR are able to reduce both thermal and mechanical hyperalgesia in a rat model of bone cancer. Third, we show that GM-CSF increases excitability of peripheral nociceptors by upregulating functional expression of nociceptor-specific Na^+ cannels, Nav1.7-Nav1.9. Furthermore, using unilateral in vivo gene knockdown we further demonstrate that Na^+ channel upregulation is indeed a necessary step in the development of GM-CSF induced pain in vivo. Finally, using a set of genetic manipulations and assays, we delineated a molecular mechanism for GM-CSF induced initiation of pain in bone cancer: up-regulation of functional Nav1.7, Nav1.8 and Nav1.9 channel activity though the Jak2-Stat3 mediated activation of Scn9a, Scn10a and Scn11a gene transcription.

Several recent studies implicated contribution of GM-CSF to different types of pain, including cancer pain, neuropathic, inflammatory and osteoarthritic pain. (Cook et al., 2012; Cook et al., 2013; Nicol et al., 2018). Yet, the exact mechanism and main molecular steps of the pro-algesic action of GM-CSF remained elusive. Our study fills this gap providing a mechanistic framework for the effect.

Increased excitability of nociceptive neurons is a fundamental mechanism for pain. In turn, changes in excitability are ultimately linked to altered ion channel

activity. Thus, in this study we focused on ion channels controlling excitability of DRG neurons. All results pinpoint Nav.7-Nav1.9 channels as key determinants of the GM-CSF proalgesic action. 1) GM-CSF increased levels of Scn9a, Scn10a and Scn11a but not the other key ion channels tested. 2) Consistent with above results, protein level of Nav1.7-Nav1.9 and the appropriate Na^+ current fractions in nociceptive DRG neurons were also increased by GM-CSF. 3) Changes of DRG neuron excitability induced by GM-CSF were consistent with elevated Na^+ channel activity: lowered rheobase, lowered threshold potential, but no significant change in resting membrane potential. Notably, GM-CSF did not change amplitude of M-type K^+ current, which is another type of ion channels, important for setting resting excitability parameters of a neuron (Table1). 4) Down regulation of Nav1.7-Nav1.9 with AS ODNs alleviated GM-CSF-induced pain behavior. While the latter evidence does not directly prove involvement of these Nav channels in GM-CSF-induced pain specifically (since down regulation of them will probably inhibit any type of pain behavior anyway), the combined evidence implicate Nav channel mechanism as the most plausible and straightforward explanation for GM-CSF induced pain nonetheless. However, contribution of other mechanisms to the GM-CSF induced pain cannot be ruled out at present; indeed involvement of other mediators, including Ccl5, Ccl3 and Il1a has been reported (Stosser et al., 2011).

We provide evidence that Jak2-Stat3 signaling pathway contributes to GM-CSF mediated up-regulation of Nav channels described above and, thus, to hyperalgesia associated with high GM-CSF levels, e.g. as observed in bone cancer. Activation of Jak by GM-CSF leads to activation of the Stat family transcription factors, which dimerize and translocate to the nucleus and modulate gene expression (Choi et al., 2011). In hematopoietic cells, GM-CSF exerts its biological functions mainly through activation of Jak2, which then activates Stat3 and Stat5 but not Stat2, Stat4 or Stat6 (Zgheib et al., 2013). However, the signal transduction pathways mediated by GM-CSF and its receptors are cell-type specific and may differ significantly (Valdembri et al., 2002). In the present study we found that in DRG neurons Jak2 and Stat3 are selectively phosphorylated following the GM-CSF treatment; phosphorylated Jak1 was not affected and phosphorylated Jak3 and Stat5 were not

fund at all. Consistent with these results, very low levels of Jak3 and Stat5 mRNA in DRG neurons were retrieved using the iBrain big data platform (Li et al., 2016). Thus, Jak2-Stat3 is likely to be the dominant signaling pathway for GM-CSF to exert its function in DRG neurons.

Luciferase reporter assay provided strong evidence indicating that Stat3 is able to bind to the promoter regions of Scn9a, Scn10a and Scn11a genes to enhance their transcription. In accordance with this observation, down-regulation of Jak2 and Stat3 with anti-sense oligodeoxynucleotides reversed the GM-CSF induced elevation of mRNA expression level of these Nav channels. Importantly, these anti-sense oligodeoxynucleotides against Scn9a-Scn11a also alleviated the GM-CSF elicited pain behavior. These results not only describe a clear mechanism for how Nav1.7-Nav1.9 channels are up-regulated by GM-CSF signaling pathway, but also indicate that specific Jak-Stat pathway could be targeted for pain therapeutics.

GM-CSF is used clinically for treatment of myelodysplastic syndromes, aplastic anemia, tumor radiotherapy and chemotherapy-induced neutropenia (Garcia et al., 2014).The most severe adverse reaction to these GM-CSF therapies is bone pain and the incidence is reported to reach up to 90% (Stosser et al., 2011). These clinical observations align very well with our results showing that GM-CSF induces pain behavior in rats when injected to DRG at a concentration of 20 ng/ml GM-CSF, which is lower than the blood concentration of after a single-dose administration of GM-CAF in humans (~600 ng/ml; (Alexanderet et al., 2016)). Thus, clinically administered GM-CSF reaches sufficient blood concentrations to be able to sensitize bone periosteal nerves and nociceptive neurons through the mechanism described here.

In summary, in this study provides mechanistic explanation for the role of GM-CSF in pain, specifically in pain associated with the bone cancer and with the GM-CSF-based therapies. This novel mechanism should be considered as a potential target for future pain treatments.

References

Alexander WS (2016). In vivo at last: Demonstrating the biological credentials and clinical potential of GM-CSF. Exp Hematol 44 (8): 669-73.

Bali KK, Venkataramani V, Satagopam VP, Gupta P, Schneider R, Kuner R (2013). Transcriptional mechanisms underlying sensitization of peripheral sensory neurons by granulocyte-/granulocyte-macrophage colony stimulating factors. Mol Pain 9: 48.

Blanchard MG, Rash LD and Kellenberger S (2012). Inhibition of voltage-gated Na(+) currents in sensory neurones by the sea anemone toxin APETx2. Br J Pharmacol 165 (7): 2167-77.

Cheng X, Dib-Hajj SD, Tyrrell L, Te MR, Drenth JP, Waxman SG (2011). Deletion mutation of sodium channel Na(V)1.7 in inherited erythromelalgia: enhanced slow inactivation modulates dorsal root ganglion neuron hyperexcitability. Brain 134 (Pt 7): 1972-86.

Choi JK, Kim KH, Park H, Park SR, Choi BH (2011). Granulocyte macrophage-colony stimulating factor shows anti-apoptotic activity in neural progenitor cells via JAK/STAT5-Bcl-2 pathway. Apoptosis 16 (2): 127-34.

Choi JS, Dib-Hajj SD, Waxman SG (2007). Differential slow inactivation and use-dependent inhibition of Nav1.8 channels contribute to distinct firing properties in IB4+ and IB4- DRG neurons. J Neurophysiol 97 (2): 1258-65.

Cook AD, Pobjoy J, Sarros S, Steidl S, Durr M, Lacey DC, Hamilton JA. (2013). Granulocyte-macrophage colony-stimulating factor is a key mediator in inflammatory and arthritic pain. Ann Rheum Dis 72 (2): 265-70.

Cook AD, Pobjoy J, Steidl S, Durr M, Braine EL, Turner AL, Hamilton JA. (2012). Granulocyte-macrophage colony-stimulating factor is a key mediator in experimental osteoarthritis pain and disease development. Arthritis Res Ther 14 (5): R199.

Cummins TR, Black JA, Dib-Hajj SD, Waxman SG (2000). Glial-derived neurotrophic factor upregulates expression of functional SNS and NaN sodium channels and their currents in axotomized dorsal root ganglion neurons. J Neurosci 20 (23): 8754-61.

de Mooij T, Wuyts W, Ham J (2012). Phenotypic Differences in Multiple Osteochondromas in Monozygotic Twins: A Case Report. JBJS Case Connect 2 (4): e60.

Dib-Hajj SD, Estacion M, Jarecki BW, Tyrrell L, Fischer TZ, Lawden M, Cummins TR, Waxman SG (2008). Paroxysmal extreme pain disorder M1627K mutation in human Nav1.7 renders DRG neurons hyperexcitable. Mol Pain 4: 37.

Du X, Gao H, Jaffe D, Zhang H and Gamper N (2018). M-type K(+) channels in peripheral nociceptive pathways. Br J Pharmacol 175 (12): 2158-2172.

Du X, Hao H, Gigout S, Huang D, Yang Y, Li L, Wang C, Sundt D, Jaffe DB, Zhang HL, Gamper N (2014). Control of somatic membrane potential in nociceptive neurons and its implications for peripheral nociceptive transmission. Pain 155 (11): 2306-22.

Du X, Hao H, Yang Y, Huang S, Wang C, Gigout S, Raml R, Li X, Jaworska E, Edwards I, Deuchars J, Yanagawa Y, Qi JL, Guan BC, Jaffe DB, Zhang HL, Gamper N (2017). Local GABAergic signaling within sensory ganglia controls peripheral nociceptive transmission. J Clin Invest 127 (5): 1741-1756.

Fortin CF, Larbi A, Dupuis G, Lesur O, Fulop TJ (2007). GM-CSF activates the Jak/STAT pathway to rescue polymorphonuclear neutrophils from spontaneous apoptosis in young but not elderly individuals. Biogerontology 8 (2): 173-87.

Francois-Moutal L, Dustrude ET, Wang Y, Brustovetsky T, Dorame A, Ju W, Moutal A, Perez-Miller S, Brustovetsky N, Gokhale V, Khanna M, Khanna R (2018). Inhibition of the Ubc9 E2 SUMO conjugating enzyme-CRMP2 interaction decreases Nav1.7 currents and reverses experimental neuropathic pain. Pain.

Garcia JA, Elson P, Tyler A, Triozzi P, Dreicer R (2014). Sargramostim (GM-CSF) and lenalidomide in castration-resistant prostate cancer (CRPC): results from a phase I-II clinical trial. Urol Oncol 32 (1): 33.e11-7.

Huang J, Han C, Estacion M, Vasylyev D, Hoeijmakers JG, Gerrits MM, Tyrrell L, Lauria G, Faber CG, Dib-Hajj SD, Merkies IS, Waxman SG (2014). Gain-of-function mutations in sodium channel Na(v)1.9 in painful neuropathy. Brain 137 (Pt 6):

1627-42.

Huang J, Vanoye CG, Cutts A, Goldberg YP, Dib-Hajj SD, Cohen CJ, Waxman SG, George AJ (2017). Sodium channel NaV1.9 mutations associated with insensitivity to pain dampen neuronal excitability. J Clin Invest 127 (7): 2805-2814.

Isensee J, Krahe L, Moeller K, Pereira V, Sexton JE, Sun X, Emery E, Wood JN, Hucho T (2017). Synergistic regulation of serotonin and opioid signaling contributes to pain insensitivity in Nav1.7 knockout mice. Sci Signal 10 (461).

Iversen PO, Rodwell RL, Pitcher L, Taylor KM, Lopez AF (1996). Inhibition of proliferation and induction of apoptosis in juvenile myelomonocytic leukemic cells by the granulocyte-macrophage colony-stimulating factor analogue E21R. Blood 88 (7): 2634-9.

Jarecki BW, Piekarz AD, Jackson JN, Cummins TR (2010). Human voltage-gated sodium channel mutations that cause inherited neuronal and muscle channelopathies increase resurgent sodium currents. J Clin Invest 120 (1): 369-78.

Lai J, Gold MS, Kim CS, Bian D, Ossipov MH, Hunter JC, Porreca F (2002). Inhibition of neuropathic pain by decreased expression of the tetrodotoxin-resistant sodium channel, NaV1.8. Pain 95 (1-2): 143-52.

Li CL, Li KC, Wu D, Chen Y, Luo H, Zhao JR, Wang SS, Sun MM, Lu YJ, Zhong YQ, Hu XY, Hou R, Zhou BB, Bao L5, Xiao HS, Zhang X (2016). Somatosensory neuron types identified by high-coverage single-cell RNA-sequencing and functional heterogeneity. Cell Research 26(1):83-102.

Li Y, North RY, Rhines LD, Tatsui CE, Rao G, Edwards DD, Cassidy RM, Harrison DS, Johansson CA, Zhang H, Dougherty PM (2018). DRG Voltage-Gated Sodium Channel 1.7 Is Upregulated in Paclitaxel-Induced Neuropathy in Rats and in Humans with Neuropathic Pain. J Neurosci 38 (5): 1124-1136.

Lilly MB, Zemskova M, Frankel AE, Salo J, Kraft AS (2001). Distinct domains of the human granulocyte-macrophage colony-stimulating factor receptor alpha subunit mediate activation of Jak/Stat signaling and differentiation. Blood 97 (6): 1662-70.

Liu B, Linley JE, Du X, Zhang X, Ooi L, Zhang H, Gamper N (2010). The acute nociceptive signals induced by bradykinin in rat sensory neurons are mediated by inhibition of M-type K+ channels and activation of Ca2+-activated Cl- channels. J Clin Invest 120 (4): 1240-52.

Lolignier S, Amsalem M, Maingret F, Padilla F, Gabriac M, Chapuy E, Eschalier A, Delmas P, Busserolles P (2011). Nav1.9 Channel Contributes to Mechanical and Heat Pain Hypersensitivity Induced by Subacute and Chronic Inflammation. PLoS ONE 6(8): e23083.

MiaoXR, GaoXF, Wu JX, Lu ZJ, Huang ZX, Li XQ, He C, Yu WF (2010). Research article Bilateral downregulation of Nav1.8 in dorsal root ganglia of rats with bone cancer pain induced by inoculation with Walker 256 breast tumor cells. BMC Cancer 10:216

Minett MS, Falk S,Sonia Santana-Varela S, Bogdanov YD, Nassar MA, Heegaard AM, Wood JN (2013). Pain without Nociceptors? Nav1.7-Independent Pain Mechanisms. Cell Reports 6(2):301-312.

Nicol L, Thornton P, Hatcher JP, Glover CP, Webster CI, Burrell M, Hammett K, Jones CA, Sleeman MA, Billinton A, Chessell I (2018). Central inhibition of granulocyte-macrophage colony-stimulating factor is analgesic in experimental neuropathic pain. Pain 159 (3): 550-559.

Qiu F, Li Y, Fu Q, Fan YY, Zhu C, Liu YH, Mi WD. (2016). Stromal Cell-Derived Factor 1 Increases Tetrodotoxin-Resistant Sodium Currents Nav1.8 and Nav1.9 in Rat Dorsal Root Ganglion Neurons via Different Mechanisms. Neurochem Res 41 (7): 1587-603.

Schweizerhof M, Stosser S, Kurejova M, Njoo C, Gangadharan V, Agarwal N, Schmelz M, Bali KK, Michalski CW, Brugger S, Dickenson A, Simone DA, Kuner R. (2009). Hematopoietic colony-stimulating factors mediate tumor-nerve interactions and bone cancer pain. Nat Med 15 (7): 802-7.

Sharma A, Oishi N, Boddicker RL, Hu G, Benson HK, Ketterling RP, Greipp PT, Knutson DL, Kloft-Nelson SM, He R, Eckloff BW, Jen J, Nair AA, Davila

JI, Dasari S, Lazaridis KN, Bennani NN, Wu TT, Nowakowski GS, Murray JA, Feldman AL (2018). Recurrent STAT3-JAK2 fusions in indolent T-cell lymphoproliferative disorder of the gastrointestinal tract. Blood 131 (20): 2262-2266.

Stosser S, Schweizerhof M, Kuner R (2011). Hematopoietic colony-stimulating factors: new players in tumor-nerve interactions. J Mol Med (Berl) 89 (4): 321-9.

Valdembri D, Serini G, Vacca A, Ribatti D, Bussolino F (2002). In vivo activation of JAK2/STAT-3 pathway during angiogenesis induced by GM-CSF. FASEB J 16 (2): 225-7.

Wang LN, Yao M, Yang JP, Peng J, Peng Y, Li CF, Zhang YB, Ji FH, Cheng H, Xu QN, Wang XY, Zuo JL (2011). Cancer-induced bone pain sequentially activates the ERK/MAPK pathway in different cell types in the rat spinal cord. Mol Pain 7: 48.

Yoneda T, Hiasa M, Nagata Y, Okui T, White F (2015). Contribution of acidic extracellular microenvironment of cancer-colonized bone to bone pain. Biochim Biophys Acta 1848 (10 Pt B): 2677-84.

Zgheib A, Pelletier-Bonnier E, Levros LJ, Annabi B (2013). Selective JAK/STAT3 signalling regulates transcription of colony stimulating factor-2 and -3 in Concanavalin-A-activated mesenchymal stromal cells. Cytokine 63 (2): 187-93.

Zheng Q, Fang D, Liu M, Cai J, Wan Y, Han JS, Xing GG (2013). Suppression of KCNQ/M (Kv7) potassium channels in dorsal root ganglion neurons contributes to the development of bone cancer pain in a rat model. Pain 154 (3): 434-48.

Figure legends

Figure 1. Role of GM-CSF in bone metastases cancer pain. (A) High expression level of GM-CSF in osteosarcoma tissue sample. H&E staining of chondroma and osteosarcoma is shown on the left; immunohistochemical staining for GM-CSF indicated by arrows in chondroma and osteosarcoma is shown on the right. **(B)** Summary results for immunohistochemical staining for GM-CSF (n = 8 per group, unpaired t-test: t=5.69, *p=0.0013). **(C)**. Effect of antibodies against GM-CSF or GM-CSFR (10 μg) and GM-CSF analogue E21R (a competitive antagonist of GM-CSF, 25 μg/μl, 3 μl) on mechanical (left panel) and thermal (right panel) nociceptive responses in bone cancer pain model of rats. The mechanical paw withdrawal threshold and thermal paw withdrawal latency were measured at 3, 7, 11, 14, 17, and 21 days for the control group (black line + squares), the bone cancer group (red line + circles), the bone cancer + antibody against GM-CSF group (blue line + triangles), the bone cancer + antibody against GM-CSFR group (pink line + triangles) and the bone cancer + E21R group (green line + triangles). Two-way ANOVA followed by Bonferroni post hoc tests revealed a significant effect of treatment ($F_{(4,150)}$=29.49, p=0) and time ($F_{(5,150)}$=5.06, p<0.0001) but no interaction between the two ($F_{(20,150)}$=0.71, p=0.81) for the left panel; a significant effect of treatment ($F_{(4,240)}$=15.10, p<0.0001), time ($F_{(4,240)}$=2.56, p=0.028) and an interaction between the two ($F_{(20,240)}$=2.20, p=0.003) for the right panel; *P < 0.05 as compared to sham group; $^{\#}$P < 0.05 with respect to the corresponding bone cancer group. **(D)** Dose-dependent effects of GM-CSF on paw withdrawal threshold to mechanical stimulus (left panel) and on paw withdrawal latency to noxious heat (right panel) at 1 h, 2 h, 5 h, 12 h and 24 h following focal DRG application via DRG cannula. Number of experiments is indicated as n in each panel. Two-way ANOVA followed by Bonferroni post hoc tests revealed a significant effect of dose ($F_{(3,345)}$=29.30, p<0.0001) but not of time ($F_{(3,345)}$=0.15, p=0.96), nor an interaction between the two ($F_{(12,345)}$=0.37, p=0.97) for the left panel. For the right panel, there was a significant effect of dose ($F_{(3,350)}$=70.95, p=0) and an interaction between dose and time ($F_{(12,350)}$=3.71, p<0.0001) but effect of time did not reach significance ($F_{(3,350)}$=2.09, p=0.08). *P < 0.05 as compared to the vehicle saline).

Figure 2. Effect of GM-CSF on the excitability of small-sized DRG neurons. (A) Representatives of action potentials evoked by depolarizing current pulse (left), recorded from small-sized DRG neurons. **(B)** Summary results for the effect of GM-CSF on numbers of action potential induced by increasing amplitudes of depolarizing currents. Two-way ANOVA followed by Bonferroni post hoc tests revealed a significant effect of treatment ($F_{(1,1057)}$=22.45, p<0.0001), injected currents ($F_{(9,1057)}$=7.82, p<0.0001) but not significant interaction between the two ($F_{(9,1057)}$=0.43, p=0.92). *P < 0.05 as compared to the control. **(C)** Single action potentials from A with expanded time scales. TP, threshold potential; RMP, rest membrane potential. **(D)** Summary results for the effect of GM-CSF on the threshold potential, rheobase current and resting membrane potential (unpaired t-test, *p<0.05 as compared to the control).

Figure 3. Effect of GM-CSF on the current amplitude and expression level of Nav1.7, Nav1.8 and Nav1.9 channels. (A) Relative mRNA expression of Nav1.7, Nav1.8, Nav1.9, Kv4.2, TMEM16A, P2X3, KCNQ2 and KCNQ3 in cultured DRG cells after incubation of GM-CSF (200 ng/ml) 24h. (n=9, unpaired t-test, *P < 0.05 as compared to the control) (B) Relative mRNA expression of Nav1.7, Nav1.8, Nav1.9 in DRG neurons of bone cancer pain at the 7th day. (n=6, unpaired t-test, *P < 0.05 as compared to the control) **(C)** Typical current traces and current density-voltage relationship of total TTX-S, TTX-R, Nav1.8 and Nav1.9 Na^+ currents in cultured DRG cells after incubation with GM-CSF (200 ng/ml) for 24h. **(D)** Western blot analysis of expression levels of Nav1.7, Nav1.8 and Nav1.9 proteins in DRG neurons treated with GM-CSF (200 ng/ml) for 18 h. (n = 3, unpaired t-test, *p<0.05 as compared to the control).

Figure 4. Down regulation of Nav1.7, Nav1.8 and Nav1.9 reverses nociceptive behavior evoked by GM-CSF. (A) Application of antisense oligodeoxynucleotides (ASO) in DRG against Nav1.7, Nav1.8 and Nav1.9 (each ASO, 12.5 μg/rat, 5μl) significantly reduced the mRNA expression level of Nav1.7, Nav1.8 and Nav1.9 increased by GM-CSF treatment, and alleviated mechanical **(B)** and thermal hyperalgesia **(C)** produced by the focal GM-CSF (200 ng) application. For (A) : (n =

6, unpaired t-test, *P < 0.05 as compared to control; #P < 0.05 with respect to the corresponding GM-CSF). For (B): two-way ANOVA followed by Bonferroni post hoc tests revealed a significant effect of treatment ($F_{(3,305)}$=109.59, p=0) but not time ($F_{(4,305)}$=0.78, p=0.54) or interaction between the two ($F_{(12,305)}$=0.65, p=0.80) for the left panel. There was a significant effect of treatment ($F_{(3,305)}$=80.53, p=0), but not time ($F_{(4,305)}$=0.20, p=0.94) or interaction between the two ($F_{(12,305)}$=0.42, p=0.95) for the middle panel. There was a significant effect of treatment ($F_{(3,335)}$=109.87, p=0), but not time $F_{(4,335)}$=0.89, p=0.47 or interaction between the two ($F_{(12,335)}$=0.37, p=0.97) for the right panel. For (C): two-way ANOVA followed by Bonferroni post hoc tests revealed a significant effect of treatment ($F_{(3,295)}$=168.25, p=0) and interaction between treatment and time ($F_{(12,295)}$=3.73, p<0.0001), but effect of time was not significant ($F_{(4,295)}$=1.34, p=0.25) for the left panel. There was a significant effect of treatment ($F_{(3,295)}$=336.23, p=0) and an interaction between treatment and time ($F_{(12,295)}$=2.04, p=0.02), but effect of time was not significant ($F_{(4,295)}$=1.05, p=0.38) for the middle panel. There was a significant effect of treatment ($F_{(3,250)}$=274.66, p=0) and interaction between treatment and time ($F_{(12,335)}$=5.38, p<0.0001), but effect of time was not significant ($F_{(4,335)}$=0.71, p=0.74) for the right panel. *P < 0.05 as compared to the vehicle saline; n=6, #P < 0.05 with respect to the corresponding GM-CSF).

Figure 5. GM-CSF increase the mRNA expression level of Nav1.7, Nav1.8, Nav1.9 channel through Jak2-Stat3 signaling pathway. (A) Relative expression of p-Jak1, p-Jak2, p-Jak3, p-stat3 and p-stat5 in DRG neurons after incubation with GM-CSF for 25 mins. (n=3, unpaired t-test, *P < 0.05 as compared to control) **(B)** Relative mRNA expression level of Nav1.7, Nav1.8, Nav1.9 in DRG neurons incubated with GM-CSF in the absence or presence of AG-490 (10 μM) and sttatic （20 μM）for 4h. (n=4-6, unpaired t-test, *P < 0.05 as compared to control; #P < 0.05 with respect to the corresponding GM-CSF). **(C)** Relative Luciferase activity in HEK 293 cells transfected with reporter vector containing Nav1.7, Nav1.8, Nav1.9 promoter regions (pGL3) co-expressed with either pcDNA3.1 (control) or pcDNA3.1-Stat3 cDNA. (n=3, unpaired t-test, *P < 0.05 as compared to control). D-F. Relative mRNA level of Nav1.7, Nav1.8, Nav1.9 in ipsilateral DRGs (L5) of rats

receiving anti-sense oligodeoxynucleotides (ASO) against different Jak and Stat signaling molecules (12.5 mg/rat, 5 μl). (n = 6, unpaired t-test, *P < 0.05 as compared to control; $^{\#}$P < 0.05 with respect to the corresponding GM-CSF). **(G-I)**. Effect of ASOs against Jak and Stat signaling molecules (12.5 mg/rat, 5 μl) on hyperalgesia responses to mechanical and thermal stimuli induced by GM-CSF. ASOs were given through the DRG cannula for 4 days and then GM-CSF (200ng) was given. For (G): two-way ANOVA followed by Bonferroni post hoc tests revealed a significant effect of treatment ($F_{(3,415)}$=125.38, p=0) but not time ($F_{(4,415)}$=0.54, p=0.70) or interaction between the two ($F_{(12,415)}$=0.73, p=0.73) for the left panel. There was a significant effect of treatment ($F_{(3,425)}$=77.18, p=0) but not time $F_{(4,425)}$=1.24, p=0.29 or interaction between the two ($F_{(12,425)}$=1.65, p=0.07) for the right panel. For (H): two-way ANOVA followed by Bonferroni post hoc tests revealed a significant effect of treatment ($F_{(3,415)}$=110.97, p=0) but not time ($F_{(4,415)}$=0.38, p=0.82) or interaction between the two ($F_{(12,415)}$=0.43, p=0.79) for the left panel. There was a significant effect of treatment ($F_{(3,440)}$=115.88, p=0) but not time ($F_{(4,440)}$=1.40, p=0.25) or interaction between the two ($F_{(12,440)}$=1.13, p=0.33) for the right panel. For (I): two-way ANOVA followed by Bonferroni post hoc tests revealed a significant effect of treatment ($F_{(3,345)}$=143.47, p=0) but not time ($F_{(4,415)}$=0.74, p=0.57) or interaction between the two ($F_{(12,415)}$=0.45, p=0.94) for the left panel. There was a significant effect of treatment ($F_{(3,440)}$=111.32, p=0) but not time ($F_{(4,440)}$=0.88, p=0.47) or an interaction between the two ($F_{(12,440)}$=0.94, p=0.50) for the right panel. n=6-8.*P < 0.05 as compared to the vehicle saline; $^{\#}$P < 0.05 with respect to the corresponding GM-CSF).

A

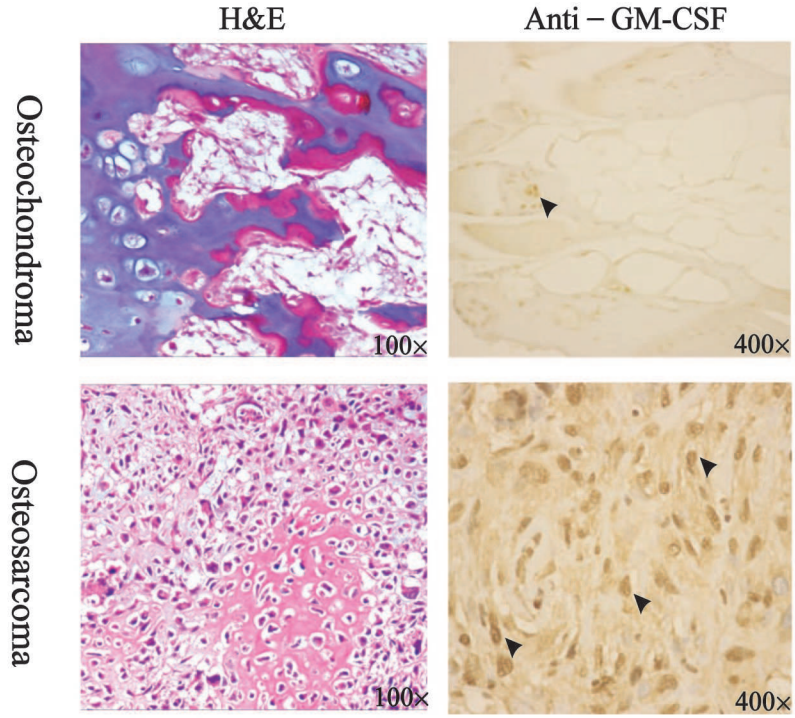
H&E
Anti – GM-CSF
Osteochondroma
Osteosarcoma
100×
400×
100×
400×

B

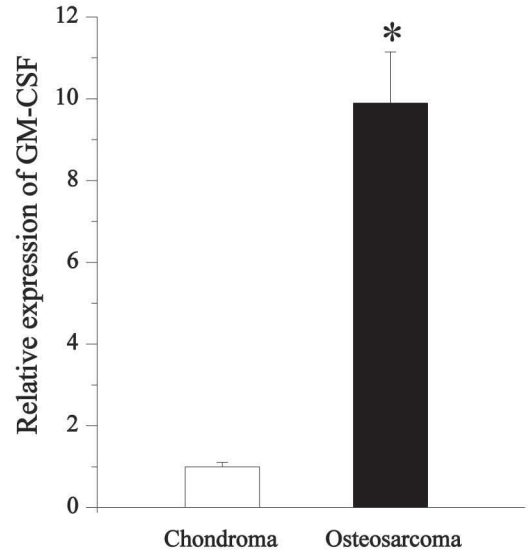
Relative expression of GM-CSF
0
2
4
6
8
10
12
*
Chondroma
Osteosarcoma

C

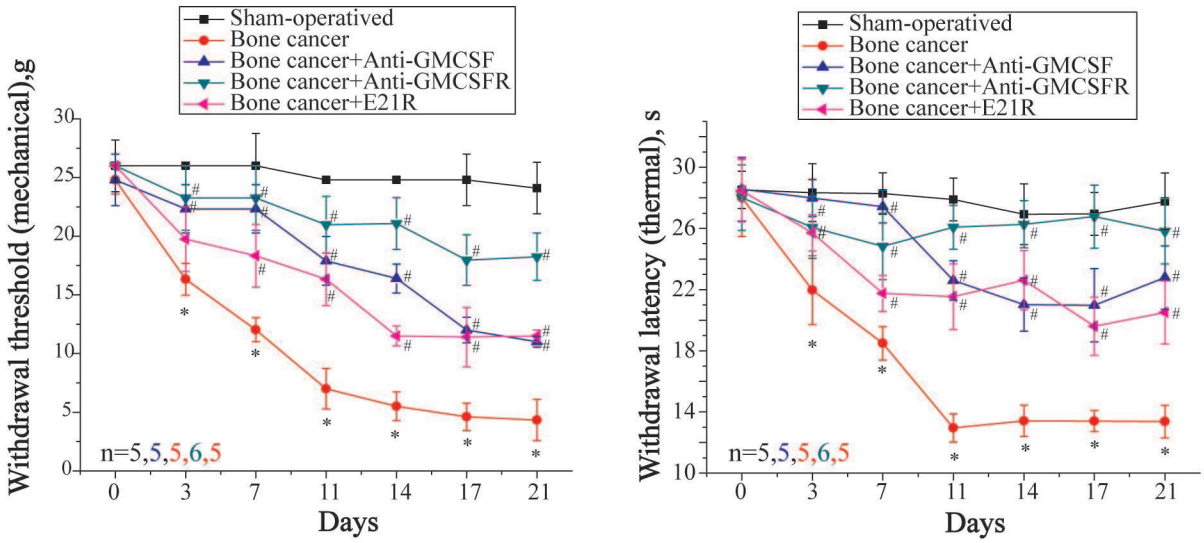
Sham-operatived
Bone cancer
Bone cancer+Anti-GMCSF
Bone cancer+Anti-GMCSFR
Bone cancer+E21R
Withdrawal threshold (mechanical),g
Withdrawal latency (thermal), s
n=5,5,5,6,5
Days
0
3
7
11
14
17
21

D

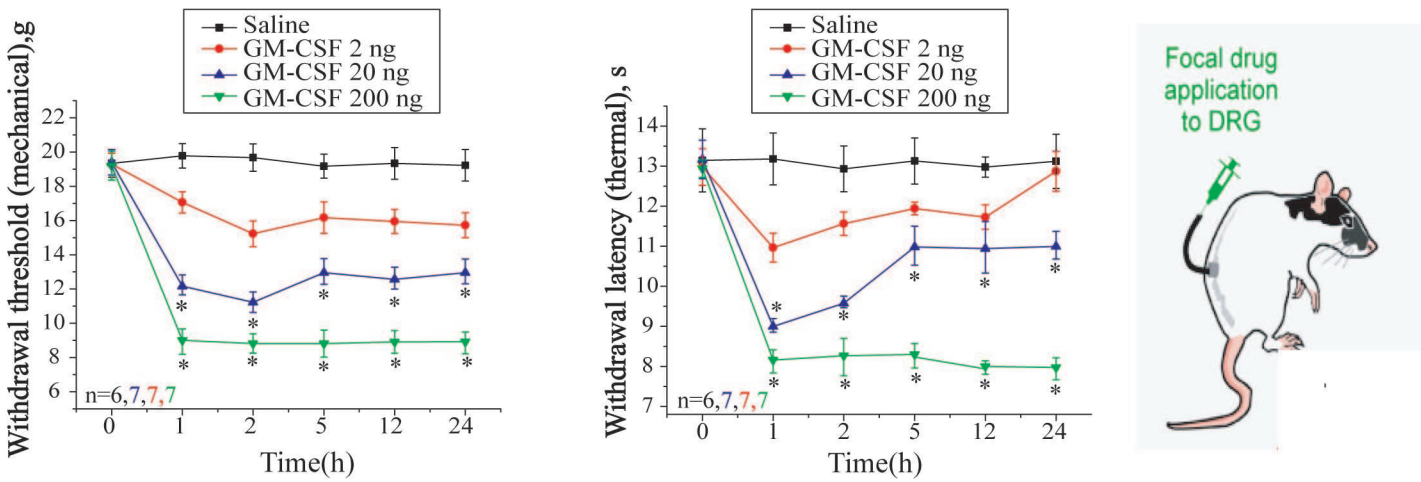
Saline
GM-CSF 2 ng
GM-CSF 20 ng
GM-CSF 200 ng
Withdrawal threshold (mechanical),g
Withdrawal latency (thermal), s
n=6,7,7,7
Time(h)
0
1
2
5
12
24
Focal drug application to DRG

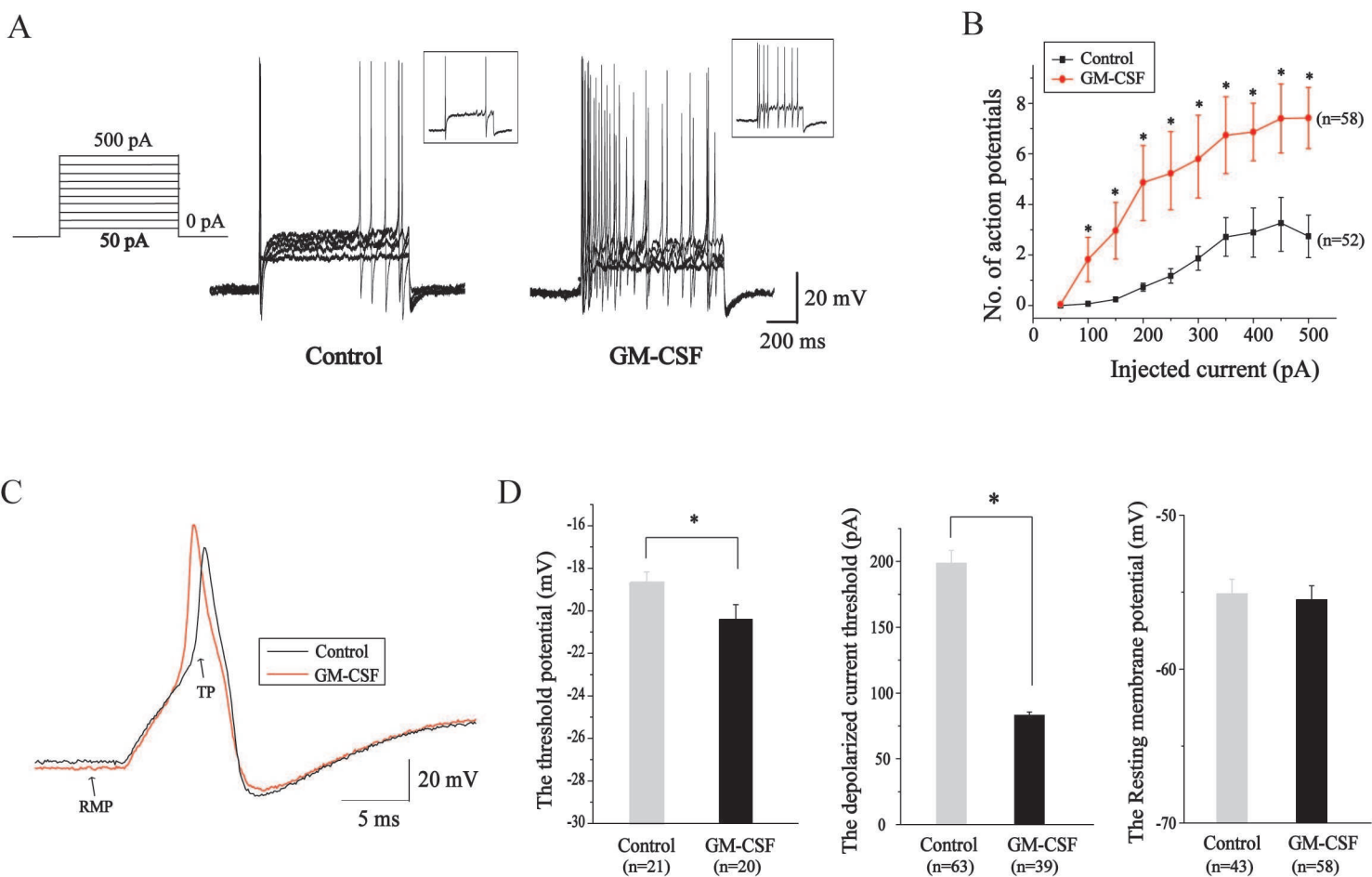
A
500 pA
0 pA
50 pA
Control
GM-CSF
20 mV
200 ms
B
Control
GM-CSF
No. of action potentials
Injected current (pA)
(n=58)
(n=52)
C
Control
GM-CSF
TP
RMP
20 mV
5 ms
D
The threshold potential (mV)
The depolarized current threshold (pA)
The Resting membrane potential (mV)
Control (n=21)
GM-CSF (n=20)
Control (n=63)
GM-CSF (n=39)
Control (n=43)
GM-CSF (n=58)

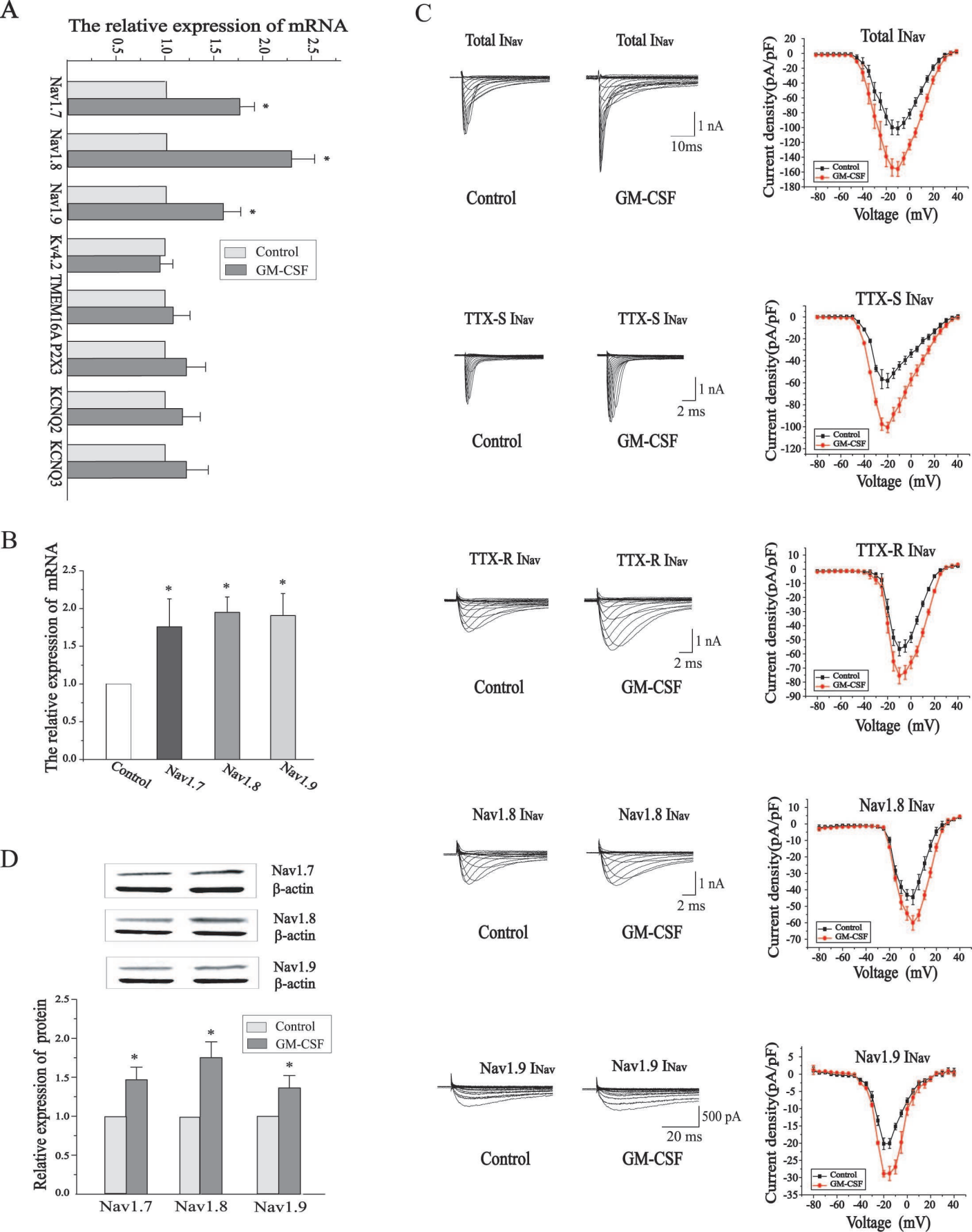
A
The relative expression of mRNA
0.5
1.0
1.5
2.0
2.5
Nav1.7
Nav1.8
Nav1.9
Kv4.2
TMEM16A
P2X3
KCNQ2
KCNQ3
Control
GM-CSF
B
The relative expression of mRNA
Control
Nav1.7
Nav1.8
Nav1.9
C
Total INav
1 nA
10ms
Control
GM-CSF
Current density(pA/pF)
Voltage (mV)
TTX-S INav
2 ms
TTX-R INav
Nav1.8 INav
Nav1.9 INav
500 pA
20 ms
D
Nav1.7
β-actin
Nav1.8
Nav1.9
Relative expression of protein

A

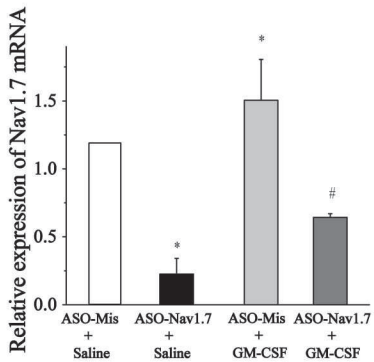
Relative expression of Nav1.7 mRNA
0.0
0.5
1.0
1.5
*
*
#
ASO-Mis + Saline
ASO-Nav1.7 + Saline
ASO-Mis + GM-CSF
ASO-Nav1.7 + GM-CSF

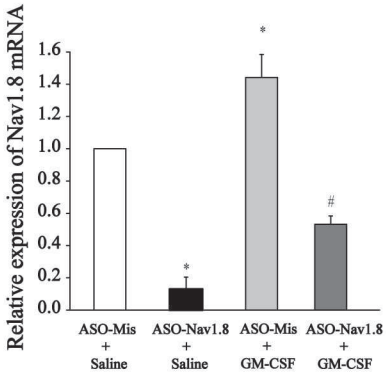
Relative expression of Nav1.8 mRNA
0.0
0.2
0.4
0.6
0.8
1.0
1.2
1.4
1.6
*
*
#
ASO-Mis + Saline
ASO-Nav1.8 + Saline
ASO-Mis + GM-CSF
ASO-Nav1.8 + GM-CSF

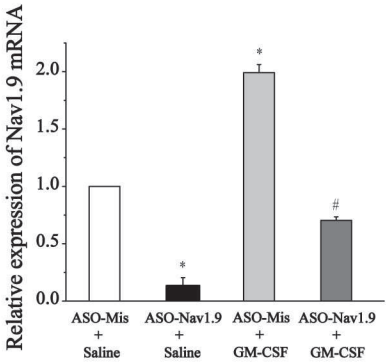
Relative expression of Nav1.9 mRNA
0.0
0.5
1.0
1.5
2.0
*
*
#
ASO-Mis + Saline
ASO-Nav1.9 + Saline
ASO-Mis + GM-CSF
ASO-Nav1.9 + GM-CSF

B

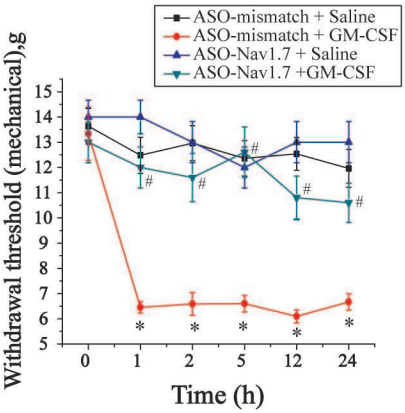
ASO-mismatch + Saline
ASO-mismatch + GM-CSF
ASO-Nav1.7 + Saline
ASO-Nav1.7 +GM-CSF
Withdrawal threshold (mechanical),g
Time (h)
0
1
2
5
12
24

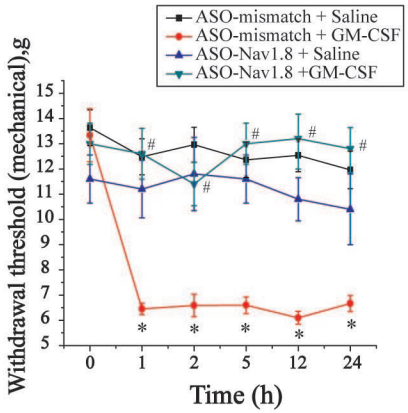
ASO-mismatch + Saline
ASO-mismatch + GM-CSF
ASO-Nav1.8 + Saline
ASO-Nav1.8 +GM-CSF
Withdrawal threshold (mechanical),g
Time (h)
0
1
2
5
12
24

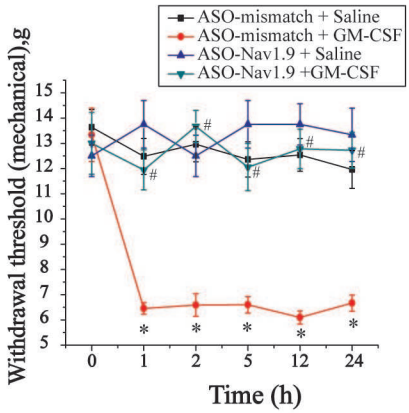
ASO-mismatch + Saline
ASO-mismatch + GM-CSF
ASO-Nav1.9 + Saline
ASO-Nav1.9 +GM-CSF
Withdrawal threshold (mechanical),g
Time (h)
0
1
2
5
12
24

C

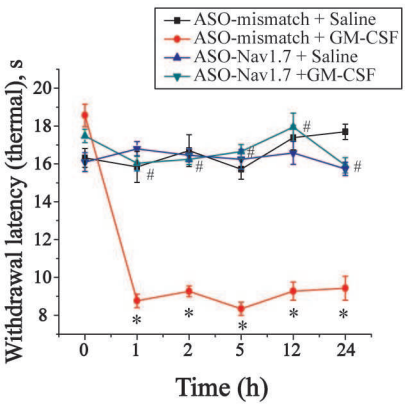
ASO-mismatch + Saline
ASO-mismatch + GM-CSF
ASO-Nav1.7 + Saline
ASO-Nav1.7 +GM-CSF
Withdrawal latency (thermal), s
Time (h)
0
1
2
5
12
24

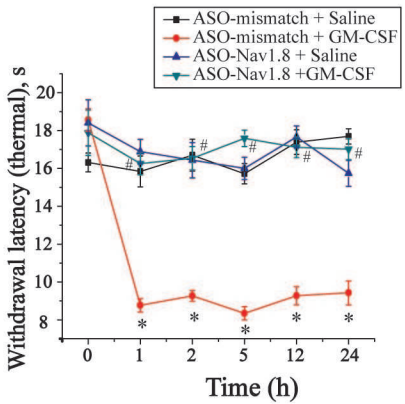
ASO-mismatch + Saline
ASO-mismatch + GM-CSF
ASO-Nav1.8 + Saline
ASO-Nav1.8 +GM-CSF
Withdrawal latency (thermal), s
Time (h)
0
1
2
5
12
24

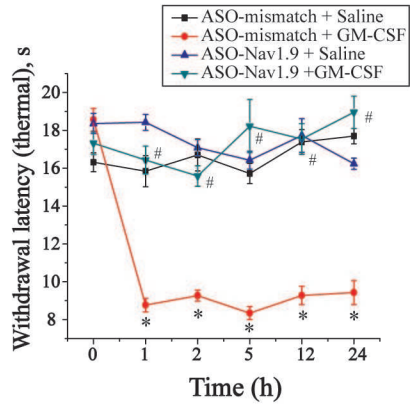
ASO-mismatch + Saline
ASO-mismatch + GM-CSF
ASO-Nav1.9 + Saline
ASO-Nav1.9 +GM-CSF
Withdrawal latency (thermal), s
Time (h)
0
1
2
5
12
24

A

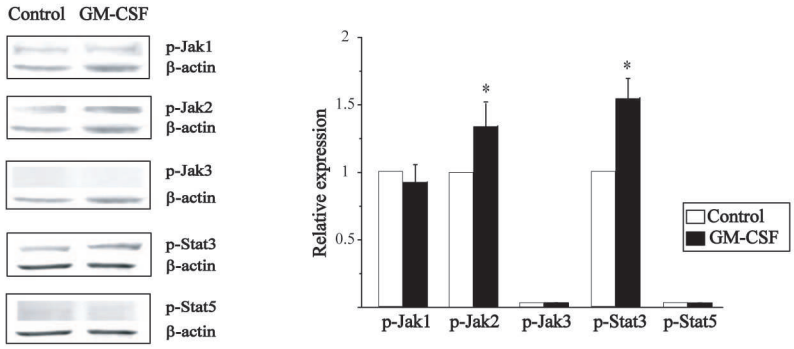
Control
GM-CSF
p-Jak1
β-actin
p-Jak2
β-actin
p-Jak3
β-actin
p-Stat3
β-actin
p-Stat5
β-actin
Relative expression
Control
GM-CSF
p-Jak1
p-Jak2
p-Jak3
p-Stat3
p-Stat5

B

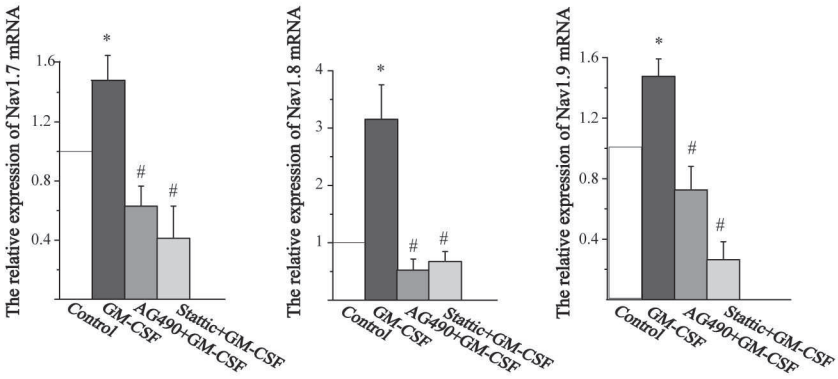
The relative expression of Nav1.7 mRNA
The relative expression of Nav1.8 mRNA
The relative expression of Nav1.9 mRNA
Control
GM-CSF
AG490+GM-CSF
Stattic+GM-CSF

C

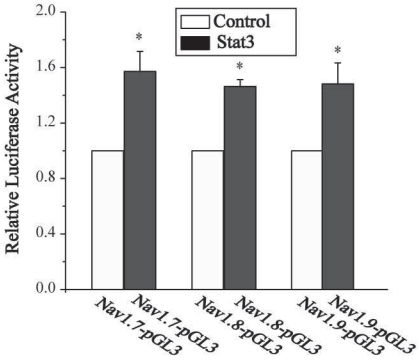
Relative Luciferase Activity
Control
Stat3
Nav1.7-pGL3
Nav1.7-pGL3
Nav1.8-pGL3
Nav1.8-pGL3
Nav1.9-pGL3
Nav1.9-pGL3

D

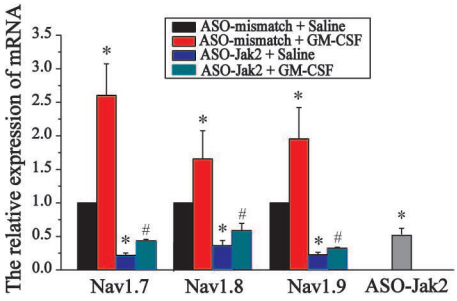
The relative expression of mRNA
ASO-mismatch + Saline
ASO-mismatch + GM-CSF
ASO-Jak2 + Saline
ASO-Jak2 + GM-CSF
Nav1.7
Nav1.8
Nav1.9
ASO-Jak2

G

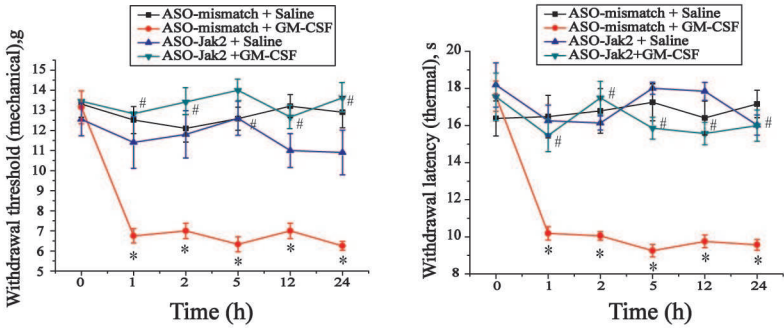
Withdrawal threshold (mechanical),g
Withdrawal latency (thermal), s
ASO-mismatch + Saline
ASO-mismatch + GM-CSF
ASO-Jak2 + Saline
ASO-Jak2 +GM-CSF
ASO-Jak2+GM-CSF
Time (h)

E

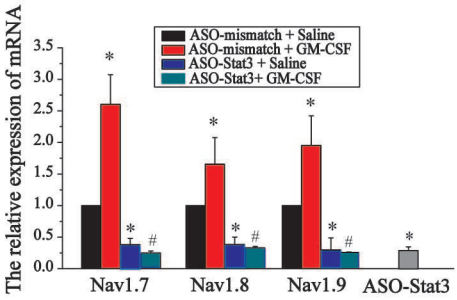
The relative expression of mRNA
ASO-mismatch + Saline
ASO-mismatch + GM-CSF
ASO-Stat3 + Saline
ASO-Stat3+ GM-CSF
Nav1.7
Nav1.8
Nav1.9
ASO-Stat3

H

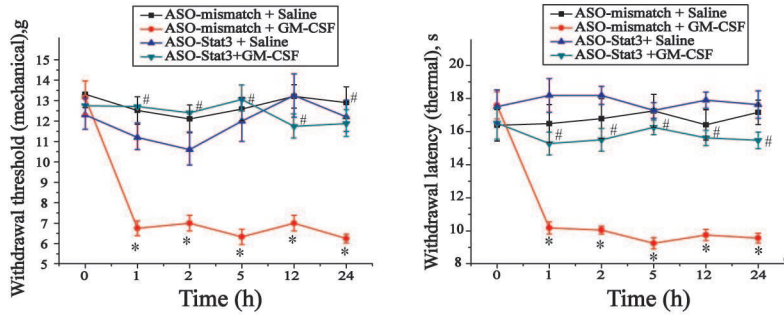
Withdrawal threshold (mechanical),g
Withdrawal latency (thermal), s
ASO-mismatch + Saline
ASO-mismatch + GM-CSF
ASO-Stat3 + Saline
ASO-Stat3+GM-CSF
ASO-Stat3+ Saline
ASO-Stat3 +GM-CSF
Time (h)

F

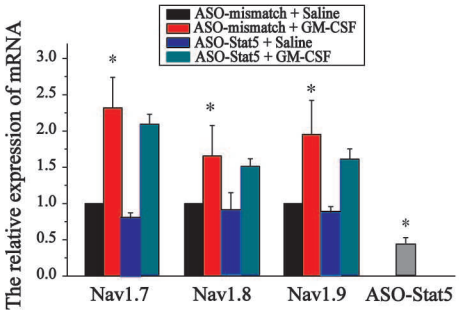
The relative expression of mRNA
ASO-mismatch + Saline
ASO-mismatch + GM-CSF
ASO-Stat5 + Saline
ASO-Stat5 + GM-CSF
Nav1.7
Nav1.8
Nav1.9
ASO-Stat5

I

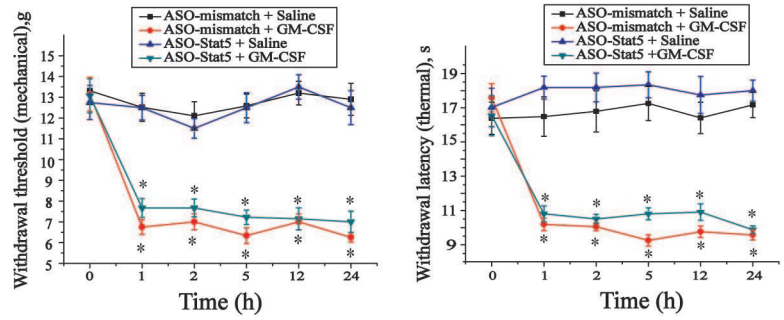
Withdrawal threshold (mechanical),g
Withdrawal latency (thermal), s
ASO-mismatch + Saline
ASO-mismatch + GM-CSF
ASO-Stat5 + Saline
ASO-Stat5 + GM-CSF
ASO-Stat5 +GM-CSF
Time (h)

Table1. Summarized effects of GM-CSF on parameters of action potential

	Rhobase currents(pA)	TP (mV)	AP amplitude (mV)	Depolariz-ation rate (v/s)	AHP amplitude（mV）	AHP duration (ms)	RMP (mV)	M-type K^+ current (pA/pF)	Rin (MΩ)
Control	198.6±9.8（63）	-18.6±0.5（23）	107.9±2.2（19）	16.2±0.6（19）	21.3±0.8（23）	19.4±0.8（18）	55.1±0.9（n=43）	3.93±1.0 (9)	564.0±51.9（32）
GM-CSF	83.1±2.5**（39）	-20.4±0.6*（22）	113.5±1.8（22）	19.3±0.4*（21）	21.6±0.8（26)	21.6±1.3（18）	55.4±0.9（58）	3.54±0.9 (8)	504.5±24.1*（25）

Rhobase currents: the depolarized current threshold for evoking the 1st action potential; TP: threshold potential; AP: action potential. RMP: resting membrane potential; Rin: input resistance. (unpaired t-test,*p<0.05, **p<0.01 compared with the control)